HHS Public Access

Author manuscript

Brain Topogr. Author manuscript; available in PMC 2017 November 12.

Published in final edited form as:

Brain Topogr. 2010 June ; 23(2): 150–158. doi:10.1007/s10548-009-0132-3.

Multimodal integration of fMRI and EEG data for high spatial and temporal resolution analysis of brain networks

D. Mantini[a,b,c], **L. Marzetti**[a,b], **M. Corbetta**[a,b,d,e], **G.L. Romani**[a,b], and **C. Del Gratta**[a,b]

[a]Dept. of Clinical Sciences and Bio-imaging, University "G. D'Annunzio", Chieti, Italy

[b]ITAB, University Foundation "G. D'Annunzio", Chieti, Italy

[c]Laboratory for Neuro-psychophysiology, K.U.Leuven Medical School, Leuven, Belgium

[c]Dept. of Neurology, Washington University, St. Louis, Missouri, USA

[d]Dept. of Radiology, Washington University, St. Louis, Missouri, USA

Abstract

Two major non-invasive brain mapping techniques, electroencephalography (EEG) and functional magnetic resonance imaging (fMRI), have complementary advantages with regard to their spatial and temporal resolution. We propose an approach based on the integration of EEG and fMRI, enabling the EEG temporal dynamics of information processing to be characterized within spatially well-defined fMRI large-scale networks. First, the fMRI data are decomposed into networks by means of spatial independent component analysis (sICA), and those associated with intrinsic activity and/or responding to task performance are selected using information from the related time-courses. Next, the EEG data over all sensors are averaged with respect to event timing, thus calculating event-related potentials (ERPs). The ERPs are subjected to temporal ICA (tICA), and the resulting components are localized with the weighted minimum norm (WMNLS) algorithm using the task-related fMRI networks as priors. Finally, the temporal contribution of each ERP component in the areas belonging to the fMRI large-scale networks is estimated. The proposed approach has been evaluated on visual target detection data. Our results confirm that two different components, commonly observed in EEG when presenting novel and salient stimuli respectively, are related to the neuronal activation in large-scale networks, operating at different latencies and associated with different functional processes.

Keywords

EEG; fMRI; independent component analysis; P300; target detection; visual oddball task

1. Introduction

Two major non-invasive brain mapping techniques, electroencephalography (EEG) and functional magnetic resonance imaging (fMRI), have complementary advantages with regard

Corresponding author: Dante Mantini, PhD, ITAB – Institute for Advanced Biomedical Technologies, "G. D'Annunzio University" Foundation, 66013 Chieti, Italy. Tel: +39-0871-3556920 Fax: +39-0871-3556930, d.mantini@unich.it.

to their spatial and temporal resolution. Recent hardware and software developments have made it feasible to acquire EEG and fMRI data simultaneously. Previous neuroimaging studies suggested that simultaneous EEG and fMRI, aiming at the fusion of the high temporal resolution of EEG and the high spatial resolution of fMRI, could be a promising way to investigate neuronal activation [Debener et al., 2005; Benar et al., 2007]. A first attempt was to use fMRI priors to estimate the contribution of the P300 sources, extracting the time-course of neuronal activation in the millisecond range [Bledowski et al., 2004; Mulert et al., 2004]. A method based on independent component analysis (ICA) was proposed for the fusion of event related potentials (ERPs) and fMRI data, jointly estimating the temporal components of the ERP response and the spatial components revealed by fMRI [Calhoun et al., 2006]. In this regard, another ICA method has been developed to match brain activity recorded by EEG and fMRI at the single-trial level [Eichele et al., 2008].

In the present study, we propose an alternative method based on ICA for the integration of EEG and fMRI data, enabling the EEG temporal dynamics of information processing to be characterized within spatially well-defined fMRI large-scale networks. We have validated the analysis method on simultaneous EEG-fMRI recordings from 13 healthy subjects, who performed a visual target detection task.

2. Materials and Methods

The EEG-fMRI analysis method for assessing the spatio-temporal dynamics of neuronal activation is illustrated in Figure 1. After the attenuation of biological and non-biological artifacts, in particular those induced by the fMRI scanning, the EEG signals are averaged, in order to obtain ERPs. A decomposition of the ERPs is performed at the group-level to highlight the event-related ICs, contributing to the neuronal processes related to task. Similarly, fMRI data are analyzed, in order to retrieve the large-scale networks accounting for the event-related responses. The fMRI network maps are used for the weighted localization of the ERP ICs, thus allowing their spatial characterization in the source space. Therefore, they are used for the analysis of neuronal activation timing across the different brain networks.

2.1. fMRI data analysis

The fMRI data are analyzed with BrainVoyager QX 1.9 (Brain Innovation, Maastricht, The Netherlands). Preprocessing steps include inter-slice time correction, motion correction, linear detrending, spatial alignment with the anatomical scans, warping into Talairach space, and spatial smoothing at 6 mm FWHM. Then, spatial independent component analysis (ICA) is applied to the fMRI single-subject data to delineate independent spatio-temporal patterns of brain activity [McKeown at al., 1998; Mantini et al., 2007b, 2009]. Data reduction by means of principal component analysis (PCA) with 60 dimensions is performed to retain at least 99.9% of the total variance. Independent components (ICs) are estimated by means of the FastICA algorithm [Hyvärinen et al., 1999]. Each fMRI-IC consists of a waveform and a spatial map: the waveform corresponds to the time-course of the specific pattern; the intensity of this activity across voxels is expressed by the associated spatial map. In order to perform group-level analysis, the ICs estimated from each subject are clustered

by means of the self-organizing group ICA (sogICA) method [Esposito et al., 2005], selecting the number of clusters equal to that of the ICs. The clusters with reproducible maps across subjects are associated with the large-scale networks active during the task. They are scaled to z-scores [Zar, 1996] and thresholded at $|z|>1.5$, in order to delineate significantly activated brain regions [Mantini et al., 2009]. Moreover, in order to isolate the fMRI networks with time-locked activity, the network time-courses are averaged with respect to the rare event onset, and a canonical hemodynamic response function (HRF), generated using a gamma function (delay time, 2 s; rise time, 4 s; fall time, 6 s; undershoot, 0.2; restore time, 2 s), is fitted to the mean time-locked response. The fMRI networks with a coefficient of determination (r-square value) larger than 0.3 are assumed to be task-related networks.

2.2. EEG data analysis

Preprocessing—The EEG recordings are referenced to the average of TP9 and TP10 channels (digitally linked mastoids reference). They are preprocessed with a modified version of the adaptive artifact subtraction (AAS) algorithm for off-line correction of imaging artifact [Gonçalves et al., 2007], downsampled to 1 kHz and filtered between 0.5 and 40 Hz, and finally subjected to the attenuation of ballistocardiographic and ocular artifacts [Mantini et al., 2007a].

Temporal ICA on ERP data—ERPs for the rare and frequent events were calculated on each dataset by averaging the artifact-corrected EEG signals with respect to their corresponding triggers (100 ms pre-stimulus and 600 ms post-stimulus time). The group-level ERPs for rare and frequent events over the scalp are obtained by computing a grand average (GA) from the individual ERPs [Goldstein et al., 2002]. Next, we used ICA on the GA, to extract the most relevant features of the event-related response, thereby increasing the contribution of time-locked brain activity and simultaneously reducing the contribution of ongoing brain activity and of noise [Makeig et al., 1997]. Accordingly, the group-level ERPs for the rare and frequent events are concatenated and subjected to temporal ICA, assuming for them different event-related temporal responses but the same source locations [Makeig et al., 1999]. The resulting ERP-ICs were classified, to exclude artifacts and noise, on the basis of the signal-to-noise ratio (SNR) and the explained variance. The SNR, defined as the ratio between the maximum amplitude in the post-stimulus interval and the root mean square (RMS) in the pre-stimulus interval, was calculated on the rare event time-course. The IC variance was measured from the IC weights provided by the ICA decomposition [James and Hesse, 2005]. The ICs with SNR larger than 10 and explained variance larger than 1% were considered salient event-related patterns of brain activity, and therefore were selected for further analyses. Finally, the amplitudes associated with the selected ERP-IC time-courses were back-reconstructed by linear projection, using information from the ERP data.

2.3. Integration of EEG and fMRI data

The spatial maps of task-related networks are used as fMRI priors in the localization of the ERP IC sensor maps, performed with the Weighted Minimum Norm Least Squares (WMNLS) algorithm [Hamalainen and Ilmoniemi, 1994] with Curry 6.0 software (Neuroscan, Hamburg, Germany). An anatomical image of the standard head from the Montreal Neurological Institute (MNI) is used for constructing the head model. In particular,

the image segmentation of the MNI head provides the surfaces used for the definition of the source space and of the realistic volume conductor model [Fuchs et al., 1998] obtained by a three compartment Boundary Element Method (BEM) model with the following conductivity values: $\sigma_{skin}=0.33Sm^{-1}$, $\sigma_{skull}=0.0042Sm^{-1}$, $\sigma_{brain}=0.33Sm^{-1}$. Moreover, the standard EEG electrode positions for source localizations is estimated by fitting the electrode montage to the skin compartment of the MNI head model. Current density maps are estimated by WMNLS in the source space, defined by a 3-dimensional regular grid with 4mm step. The brain areas included in all the task-related fMRI network maps are segmented, dilated by 5mm to account for the difference between electrophysiological and hemodynamic activity, and weighted at 140% with respect to all other locations [Liu et al., 1998]. The average EEG power in each area belonging to the fMRI networks is used for evaluating the spatial distribution of the sources associated with the ERP-IC time-course. For each ERP-IC, the noise level across the brain, calculated projecting to the source space the sensor covariance matrix of the noise, is used to scale the spatial maps to z-scores [Dale et al., 2000]. Finally, the statistical significance of the ERP activations is performed by means of permutation testing [Maris and Oostenveld, 2007].

2.4. Application to target detection data analysis

The method was applied to simultaneous EEG-fMRI recordings from 13 healthy subjects (all right-handed males, age 19–26 years). The study was approved by the local Institutional Ethics Committee. All participants signed a written informed consent before the experiment. They performed a visual oddball task. The stimuli were yellow (frequent events, 80% presentation times) and blue disks (rare events, 20% presentation times), appearing on a black background with 200 ms duration, and randomly presented every 2500 ms. The acquisition lasted about 8 minutes, for a total of 154 frequent and 38 rare events.

fMRI acquisitions were performed using a 1.5 T Siemens Magnetom Vision Scanner with a standard quadrature head coil. Functional images were acquired by means of T2*-weighted echo planar imaging (EPI) free induction decay (FID) sequences with the following parameters: TE 60 ms, matrix size 64 × 64, FOV 256 mm, in-plane voxel size 4 mm × 4 mm, flip angle 90°, slice thickness 7 mm and no gap. Each fMRI volume, acquired with a volume TR of 2500 ms and a scan time of 1620 ms, consisted of 16 bicommissural slices covering the whole brain, and its onset was time-locked to the visual stimulus presentation. After the functional study, a high resolution structural volume was acquired via a 3D MPRAGE sequence (sagittal slices, matrix 256 × 256, FOV 256 mm, slice thickness 1 mm, no gap, in-plane voxel size 1 mm × 1 mm, flip angle 12°, TR = 9.7 ms, TE = 4 ms) in order to provide the anatomical reference for the functional scans.

A 32-channel MR-compatible BrainAmp system (Brainproducts, Munich, Germany) was used for the EEG acquisition. All the electrodes, integrated into the cap, were ring-type sintered nonmagnetic Ag/AgCl electrodes. Twenty-nine EEG electrodes were placed on the scalp according to the 10% system. The physical reference electrode was the Fcz electrode, located between electrodes Fz and Cz. An additional electrode was dedicated to electrocardiogram (EKG), and two other electrodes to electrooculogram (EOG1 and EOG2). An electrode paste (ABRALYT 2000) was used for ensuring current conduction,

maintaining the impedance of each electrode close to 5 kΩ. EEG data were collected in the band 0.016–250 Hz with a sampling rate of 5 kHz.

3. Results

The ICA-based analysis of fMRI data provided a number of independent spatio-temporal patterns. We identified five fMRI networks, which were consistently found across all subjects (Figure 2). Their spatial maps were essentially coextensive with the dorsal attention, the ventral attention, the core, the visual and the sensory-motor networks, as previously defined in neuroimaging studies on active and passive behavioral tasks [Corbetta and Shulman, 2002; Dosenbach et al., 2006; Fox et al., 2006; Nir et al., 2006]. The ventral attention network is typically related to target detection processes and mainly includes the right temporo-parietal junction, inferior and middle frontal gyrus, and anterior cingulate. The dorsal attention network is associated with orienting of attention, and primarily includes the intraparietal sulcus, the frontal eye field (FEF), and the middle frontal gyrus. The core network is dedicated to task control and includes the anterior cingulate, the bilateral insular and dorso-lateral prefrontal cortices. The visual network includes the retinotopic occipital cortex and temporal-occipital regions dedicated to visual processing. The sensory-motor network includes the precentral, postcentral, and medial frontal gyri, the primary sensory-motor cortices, and the supplementary motor area. Among these five networks, we detected the visual, the core and the ventral attention networks to be time-locked to the rare event presentation, and therefore to be related to the oddball task execution (Figure 2).

After averaging EEG data with respect to rare events, we observed an ERP waveform in the 300–400 ms range, mostly distributed over the centro-parietal region, and largely corresponding to the P300 component (Figure 3). Conversely, it was more complicated to distinguish the P2 component, more frontal and early (at around 250 ms) with respect to the P3 component. In addition, we also detected the visual N1 component at the latency of about 85 ms. Nonetheless, the direct source localization of the ERP response to rare events seemed not to adequately show the different sources activated by task execution (Figure 3). Particularly, localization at 85 ms did not include primary visual areas in the occipital regions, but mainly parietal and temporal areas.

The ICA decomposition of the ERP data evidenced five ERP-ICs with different spatial and temporal profiles, accounting for the event-related responses. For each of them, the time-courses related to the rare and frequent events, the sensor map and the bar plot of the source power z-scores in the task-related network areas were estimated (Figure 4). The results obtained with the use of fMRI priors seemed to resolve the contribution of the ERP-ICs to the different networks [Liu et al., 1998]. In particular, the contribution of the visual areas could be clearly detected. We observed that the visual network was mostly involved in sensory processing, with a response at about 90 ms; the core network showed a response between 200 and 250 ms (P2 component), that could be related to task monitoring [Dosenbach et al., 2006]; the ventral attention network showed brain responses between 280 and 350 ms (P3 component), that could be ascribed to change detection and related memory processes [Corbetta and Shulman, 2002].

4. Discussion

We further demonstrated, in this study, the effectiveness of the multimodal integration of fMRI and EEG data for high spatial and temporal resolution analysis of brain network activity. Aiming at improving the accuracy of the estimated sources with respect to direct ERP localization, a number of integrated methods based on EEG and fMRI data had been already proposed. From this standpoint, the most common approach is based on the use of spatial constraints, where information from the location of fMRI activation is used for event-related potential (ERP) source reconstruction [Bledowski et al., 2004; Mulert at al., 2004].

In EEG-fMRI studies, ICA was previously proposed by Calhoun, for direct ERP-fMRI fusion [Calhoun et al., 2006], and by Eichele, for single-trial EEG-fMRI matching [Eichele et al., 2008]. In particular, Calhoun suggested to fuse the electromagnetic temporal information in the ERP with data the hemodynamic spatial information in the fMRI data by using the joint constraints of ERP and fMRI independence in the ICA model. This approach, although proven to be valuable in the study of time-locked activity, might not be suitable to provide a description of the activation timing across distinct brain networks. Alternatively, Eichele proposed to perform ICA separately on EEG and fMRI data, and to match the ICs that are consistent across modalities on the basis of their trial-to-trial variations. This approach may reveal interesting correspondences between electrophysiological and hemodynamic measures [Heeger and Ress, 2002]; on the other hand, it might be sensitive to an incomplete matching between the EEG and fMRI time-courses associated with the same generators.

Our method is intended to provide a high resolution spatio-temporal analysis of how activations propagate at different latencies across the networks engaged by the task. We analyze fMRI images according to a data-driven approach by means of ICA, a signal processing method able to separate independent spatio-temporal patterns of brain activity [McKeown et al., 1998]. We also extract with ICA the most prominent features from the ERP data, and we localize them within the areas of the time-locked fMRI networks. Accordingly, the method is not likely to be biased by the use of an incomplete model for the fusion of EEG and fMRI data, although similar spatial distribution of the EEG and fMRI sources is assumed in our method. Nonetheless, inter-individual differences in electrode locations, and in cortex and volume conductor geometry, may possibly result in the blurring of EEG inverse solutions, in turn yielding an overall decreased spatial resolution.

For the validation of the method, we analyzed data collected in a visual oddball task. In a previous study, the same data had been used to investigate the trial-to-trial changes of P300 intensity [Mantini et al., 2009], without taking into account the latency of the P300 component. Conversely, the intensity changes across trials are cancelled out by averaging with the proposed EEG-fMRI method, whereas the difference in latency of the different ERP components is investigated. The application of the method to visual oddball data provided a high-resolution spatio-temporal characterization of the P300 neuronal activations across distinct cortical networks. We observed that the detection of rare targets stimulated a complex limbic-parieto-frontal system, involving the visual, the core and the ventral attention networks. The differences found in the activation timing across their areas confirm

that different brain functions could be dynamically engaged, and can be related to the different ERP components elicited by the oddball task.

It is our opinion that the described ICA-based approach may be extended to more complex experimental paradigms, and could be also proposed for the integration of fMRI and magnetoencephalography (MEG) data.

Acknowledgments

The authors wish to thank Simone Cugini and Mauro Gianni Perrucci for technical assistance and data acquisition. Dante Mantini was partly supported by the Research Foundation Flanders (FWO).

References

Benar CG, Schon D, Grimault S, Nazarian B, Burle B, Roth M, Badier JM, Marquis P, Liegeois-Chauvel C, Anton JL. Single-trial analysis of oddball event-related potentials in simultaneous EEG-fMRI. Hum Brain Mapp. 2007; 28:602–613. [PubMed: 17295312]

Bledowski C, Prvulovic D, Goebel R, Zanella FE, Linden DE. Attentional systems in target and distractor processing: a combined ERP and fMRI study. Neuroimage. 2004; 22:530–540. [PubMed: 15193581]

Calhoun VD, Adali T, Pearlson GD, Kiehl KA. Neuronal chronometry of target detection: fusion of hemodynamic and event-related potential. Neuroimage. 2006; 30:544–553. [PubMed: 16246587]

Corbetta M, Shulman GL. Control of goal-directed and stimulus-driven attention in the brain. Nat Rev Neurosci. 2002; 3:201–215. [PubMed: 11994752]

Dale AM, Liu AK, Fischl BR, Buckner RL, Belliveau JW, Lewine JD, Halgren E. Dynamic Statistical Parametric Neurotechnique Mapping: Combining fMRI and MEG for High-Resolution Imaging of Cortical Activity. Neuron. 2000; 26:55–67. [PubMed: 10798392]

Debener S, Ullsperger M, Siegel M, Fiehler K, von Cramon DY, Engel AK. Trial-by-trial coupling of concurrent electroencephalogram and functional magnetic resonance imaging identifies the dynamics of performance monitoring. J Neurosci. 2005; 25:11730–11737. [PubMed: 16354931]

Dosenbach NU, Visscher KM, Palmer ED, Miezin FM, Wenger KK, Kang HC, Burgund ED, Grimes AL, Schlaggar BL, Petersen SE. A core system for the implementation of task sets. Neuron. 2006; 50:799–812. [PubMed: 16731517]

Eichele T, Calhoun VD, Moosmann M, Specht K, Jongsma ML, Quiroga RQ, Nordby H, Hugdahl K. Unmixing concurrent EEG-fMRI with parallel independent component analysis. Int J Psychophysiol. 2008; 67:222–234. [PubMed: 17688963]

Esposito F, Scarabino T, Hyvärinen A, Himberg J, Formisano E, Comani S, Tedeschi G, Goebel R, Seifritz E, Di Salle F. Independent component analysis of fMRI group studies by self-organizing clustering. Neuroimage. 2005; 25:193–205. [PubMed: 15734355]

Fox MD, Snyder AZ, Zacks JM, Raichle ME. Coherent spontaneous activity accounts for trial-to-trial variability in human evoked brain responses. Nat Neurosci. 2006; 9:23–25. [PubMed: 16341210]

Fuchs M, Drenckhahn R, Wischmann HA, Wagner M. An improved boundary element method for realistic volume-conductor modeling. IEEE Trans Biomed Eng. 1998; 45:980–997. [PubMed: 9691573]

Goldstein A, Spencer KM, Donchin E. The influence of stimulus deviance and novelty on the P300 and novelty P3. Psychophysiology. 2002; 39:781–790. [PubMed: 12462506]

Gonçalves SI, Pouwels PJ, Kuijer JP, Heethaar RM, de Munck JC. Artifact removal in co-registered EEG-fMRI by selective average subtraction. Clin Neurophysiol. 2007; 118:2437–2450. [PubMed: 17889599]

Hamalainen MS, Ilmoniemi RJ. Interpreting magnetic fields of the brain: minimum norm estimates. Med Biol Eng Comput. 1994; 32:35–42. [PubMed: 8182960]

Heeger DJ, Ress D. What does fMRI tell us about neuronal activity? Nat Rev Neurosci. 2002; 3:142–151. [PubMed: 11836522]

Hyvärinen A. Fast and robust fixed-point algorithms for independent component analysis. IEEE Trans Neural Network. 1999; 10:626–634.

James CJ, Hesse CW. Independent component analysis for biomedical signals. Physiol Meas. 2005; 26:R15–R39. [PubMed: 15742873]

Liu AK, Belliveau JW, Dale AM. Spatiotemporal imaging of human brain activity using functional MRI constrained magnetoencephalography: Monte Carlo simulations. Proc Nat Acad Sci USA. 1998; 95:8945–8950. [PubMed: 9671784]

Makeig S, Westerfield M, Townsend J, Jung TP, Courchesne E, Sejnowski TJ. Functionally independent components of early event-related potentials in a visual spatial attention task. Philos Trans R Soc Lond B Biol Sci. 1999a; 354:1135–1144. [PubMed: 10466141]

Mantini D, Perrucci MG, Cugini S, Ferretti A, Romani GL, Del Gratta C. Complete artifact removal for EEG recorded during continuous fMRI using independent component analysis. Neuroimage. 2007a; 34:598–607. [PubMed: 17112747]

Mantini D, Perrucci MG, Del Gratta C, Romani GL, Corbetta M. Electrophysiological signatures of resting state networks in the human brain. Proc Natl Acad Sci U S A. 2007b; 104:13170–13175. [PubMed: 17670949]

Mantini D, Corbetta M, Perrucci MG, Romani GL, Del Gratta C. Large-scale brain networks account for sustained and transient activity during target detection. Neuroimage. 2009; 44:265–274. [PubMed: 18793734]

Makeig S, Jung TP, Bell AJ, Ghahremani D, Sejnowski TJ. Blind separation of auditory event-related brain responses into independent components. Proc Natl Acad Sci USA. 1997; 94:10979–10984. [PubMed: 9380745]

Maris E, Oostenveld R. Nonparametric statistical testing of EEG- and MEG-data. J Neurosci Methods. 2007; 164:177–190. [PubMed: 17517438]

McKeown MJ, Makeig S, Brown GG, Jung TP, Kindermann SS, Bell AJ, Sejnowski TJ. Analysis of fMRI data by blind separation into independent spatial components. Hum Brain Mapp. 1998; 6:160–188. [PubMed: 9673671]

Mulert C, Jager L, Schmitt R, Bussfeld P, Pogarell O, Moller HJ, Juckel G, Hegerl U. Integration of fMRI and simultaneous EEG: towards a comprehensive understanding of localization and time-course of brain activity in target detection. Neuroimage. 2004; 22:83–94. [PubMed: 15109999]

Nir Y, Hasson U, Levy I, Yeshurun Y, Malach R. Widespread functional connectivity and fMRI fluctuations in human visual cortex in the absence of visual stimulation. Neuroimage. 2006; 30:1313–1324. [PubMed: 16413791]

Zar, JH. Biostatistical Analysis. Prentice-Hall; Upper Saddle River, NJ: 1996.

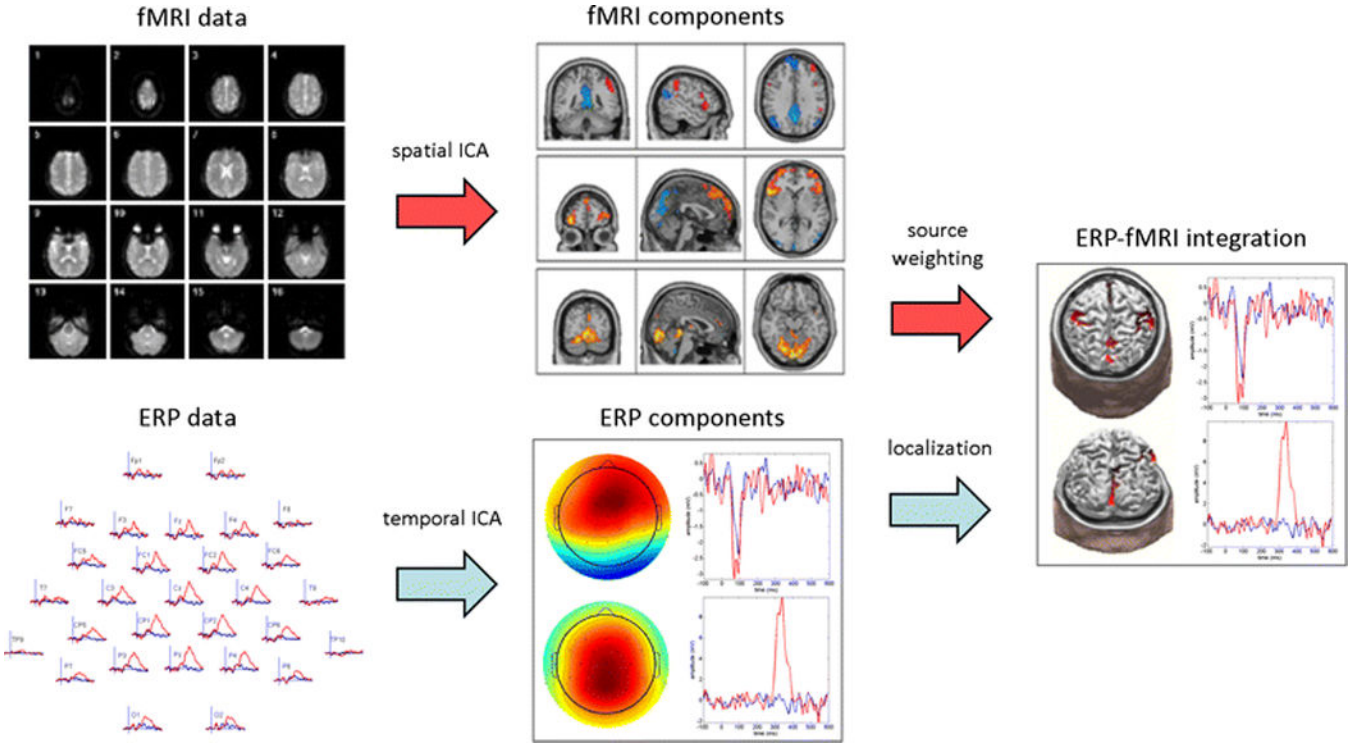

Figure 1.

Schematic representation of the analysis used for linking ERP activity and fMRI networks. The azure and red arrows illustrate the steps for EEG and fMRI data analysis, respectively. The ERP data are processed with temporal ICA, to detect independent neuronal activations. The fMRI data were analyzed with spatial ICA, to identify the spatial distribution of large-scale networks. Finally, for each ERP IC scalp map, source localization is performed jointly using the spatial maps of task-related networks as fMRI priors.

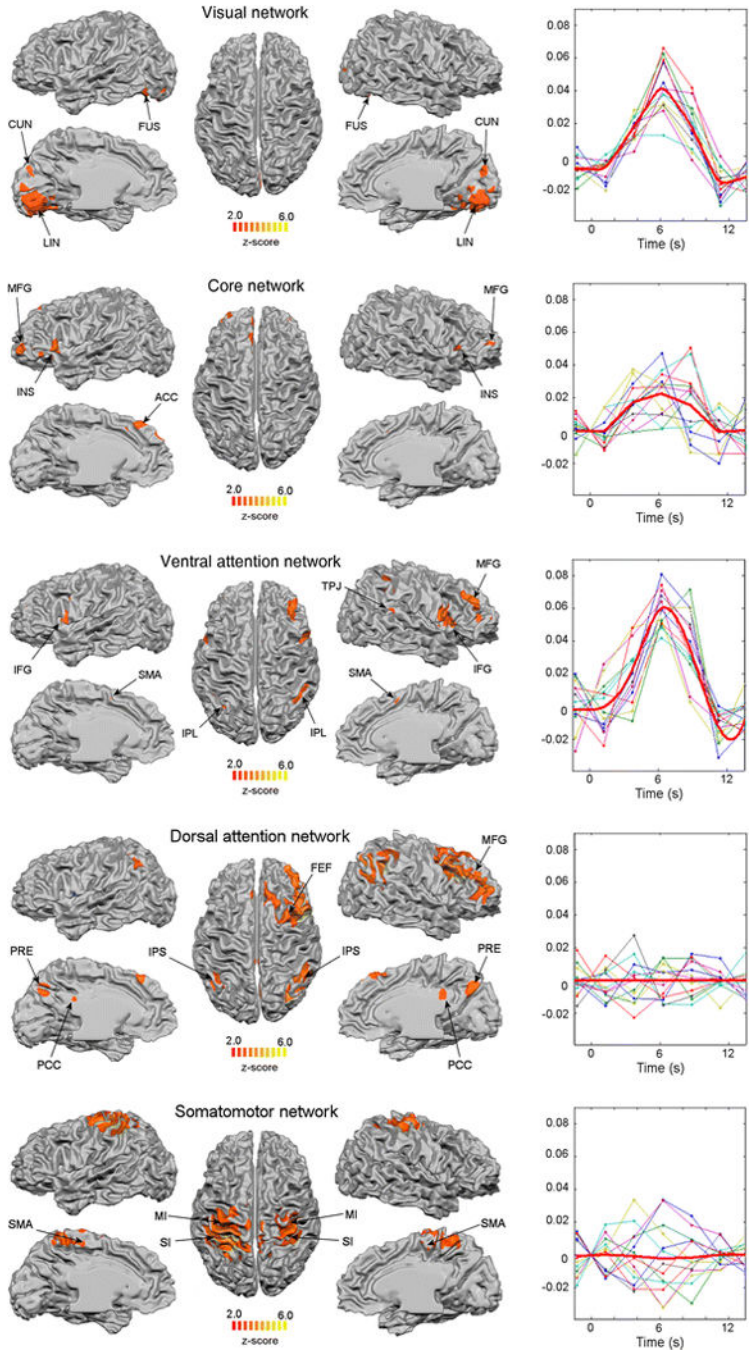

Figure 2.

Spatio-temporal analysis of the five networks consistently found across subjects, which spatially overlap with the dorsal attention, the ventral attention, the core, the visual and the sensory-motor networks. For each network, the cortical representation is shown (left panel), along with the time-course in response to rare events (right panel). The average time-courses are normalized because they refer to the average activity of the brain patterns. The thick red line in each graph represents the hemodynamic response function (HRF) best-fit to all data points. (CUN=cuneus; LIN=lingual gyrus; FUS=fusiform gyrus; INS=insula; ACC=anterior

cingulate; MFG=middle frontal gyrus; IFG=inferior frontal gyrus; SMA=supplementary motor area; TPJ=temporoparietal junction; IPL=intraparietal lobule; IPS=intraparietal sulcus; FEF=frontal eye field; PRE=precuneus; PCC=posterior cingulate; MI=primary motor area; SI=primary somatosensory area).

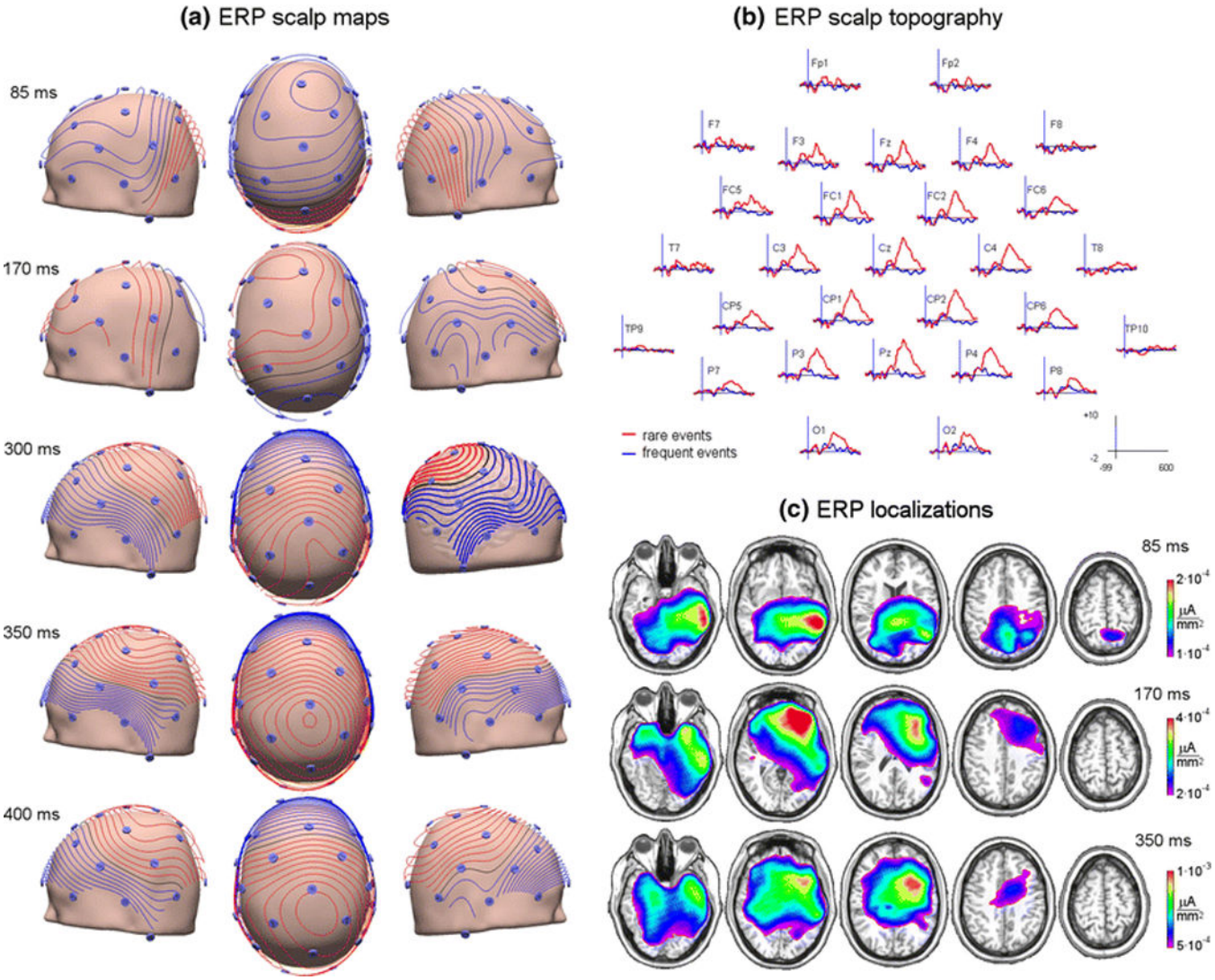

Figure 3.

ERP analysis of the grand average signals. (a) Scalp maps showing the temporal evolution of the ERP response to rare events; (b) Scalp topography of ERPs associated with rare and frequent events, colored in red and blue respectively; (c) Source distribution for rare-event ERP by WMNLS localization.

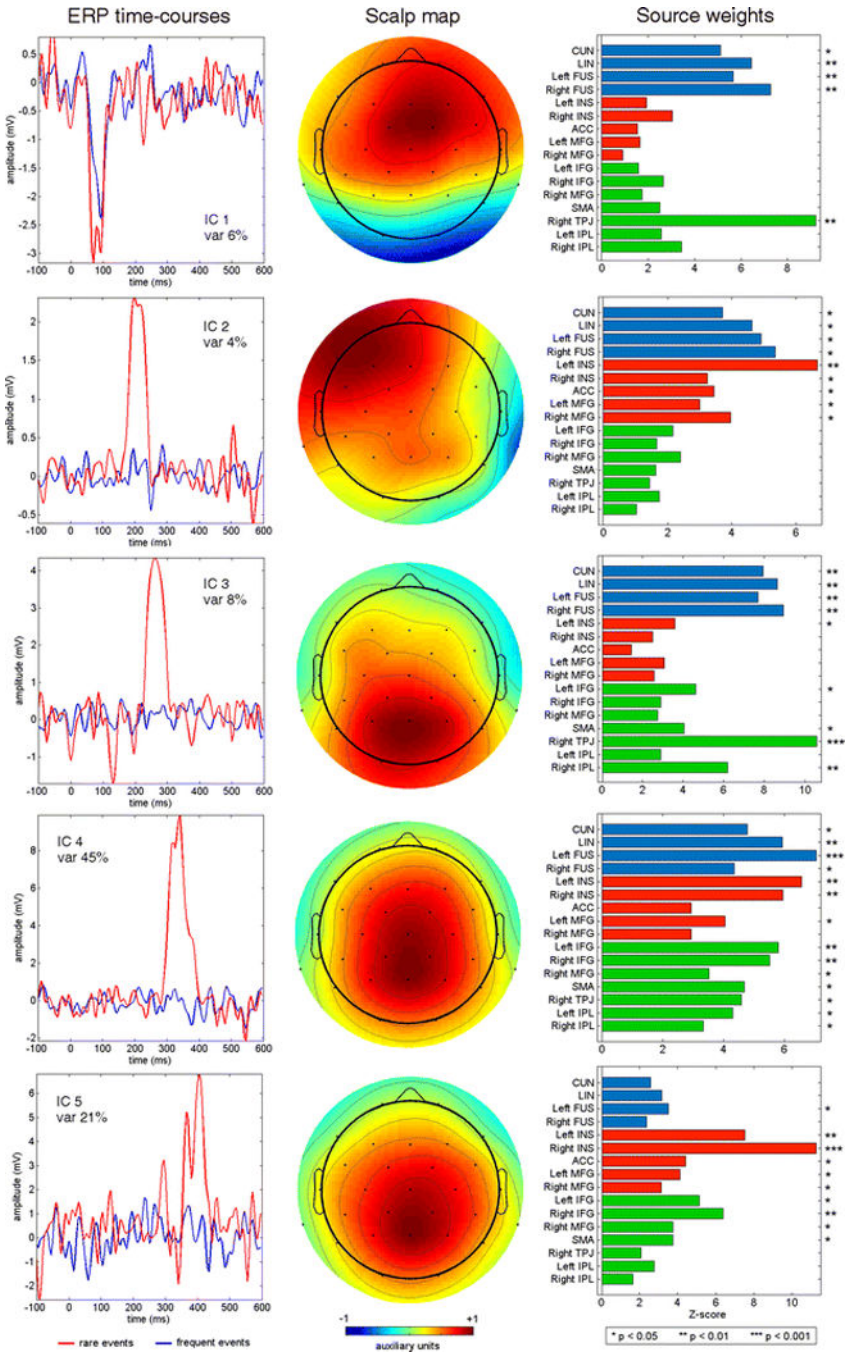

Figure 4.

Spatio-temporal analysis of the detected ERP ICs. For each IC, the time-domain response to rare and frequent events, the scalp map, and the normalized source power in the main areas of the visual, the core and the ventral attention networks (in blue, red and green colors respectively) are shown. The statistical significance of the ERP-ICs across the brain areas is also provided. (CUN=cuneus; LIN=lingual gyrus; FUS=fusiform gyrus; INS=insula;

ACC=anterior cingulate; MFG=middle frontal gyrus; IFG=inferior frontal gyrus; SMA=supplementary motor area; TPJ=temporoparietal junction; IPL=intraparietal lobule).